

## **Significance of Creep-Fatigue Interactions in Structural Integrity Assessment**

**K. BHANU SANKARA RAO AND A. NAGESHA**

*Indira Gandhi Centre for Atomic Research, Kalpakkam - 603 102*

### **ABSTRACT**

Creep-fatigue interaction is a special phenomena that have a detrimental effect on the performance of metal parts of components operating at elevated temperatures. This paper deals with the simultaneous interactions between creep and fatigue. The effect of hold time, hold position, temperature and creep ductility on creep-fatigue interaction life and damage modes of several high temperature alloys are presented in detail. The inherent deficiencies and potentially serious consequences of over-or under- design by using the classical Linear Time and Cycle-Fraction rule for predicting structural durability under high temperature creep-fatigue conditions are presented. The potential of a strain based approach in accurately predicting creep-fatigue life for ensuring structural integrity is outlined.

### **INTRODUCTION**

Creep-fatigue interaction is a special phenomena that can have a detrimental effect on the performance of metal parts of components operating at elevated temperatures. When temperatures are high enough, time dependent creep strains as well as cyclic (fatigue) strains can be present; interpretation of the effect that one has on the other becomes extremely important. For example, it has been found that creep strains can seriously reduce fatigue life and/or that fatigue strains can seriously reduce creep life. It is the quantification of these effects and the application of this information to life prediction procedures that constitutes the primary objective in creep-fatigue interaction [1].

Creep and fatigue damage interactions may occur during either isothermal or nonisothermal (thermal or thermomechanical) cyclic loading at elevated temperatures. Historically, the effects of creep-fatigue interaction in metals and alloys have usually been studied under simpler, less expensive isothermal laboratory conditions for ease of interpretation of results. This course of action has been justifiable on the basis that service-induced loading, although nonisothermal on a complete cycle basis, are nominally isothermal for extended periods of time during which creep or relaxation occurs. Hence, isothermal creep-fatigue studies are really a subset of the more general thermomechanical creep-fatigue interaction problem.

“It is not satisfactory to assess the safety of the structures in terms of fatigue or creep alone since the presence of one phenomenon may lower the limit of the other”.

Several questions arise when the specifics of this statement are studied. The suggestion that the presence of one phenomenon may lower the limit implies that the limit may or may not be lowered. What determines how much the limit is lowered? What is meant by the limit and how is it quantified?

Most experimental studies of creep-fatigue behaviour are aimed to answer these questions and to develop a basic understanding of this behaviour. Such understanding is closely linked to the evaluation of damage mechanisms and failure modes and to the development of life prediction methods. This would enable the boundaries between the different damage modes to be established. It is important to know these boundaries, since any extrapolation of short term data is only valid provided it remains within one failure regime. These methods outline the principles to be applied in prediction the expected operating life when a component is subjected to a creep influence of a certain magnitude in the presence of a fatigue influence of a certain magnitude.

## **CREEP-FATIGUE INTERACTION**

### *Conceptual Mechanisms*

Creep-fatigue interactions may be classified into two categories according to how the damage is applied. In sequential interactions, the fatigue and creep-fatigue damage modes are separate and follow each other, whereas in "simultaneous" interactions an element of each damage mode exists in every strain (or stress) cycle [2].

Simultaneous interactions have been widely investigated using strain controlled cycling with hold periods inserted at either the tensile or compressive half of the cycle, or both, such that a creep component is systematically introduced into a fatigue cycle (Fig. 1). Slow-fast and fast-slow tests were also employed for studying creep-fatigue interactions.

Generally, in the case of austenitic stainless steels, it has been established that at relatively high temperatures, continuous cycling fatigue endurance degrades when a hold period is included in the cycle. Furthermore, the imposition of holds in the tension side of the hysteresis loop tended to be more deleterious than those imposed on the compression side, (Fig. 2), and hold periods introduced at peak tensile strains are found significantly damaging than the hold periods introduced at other locations in the hysteresis loops [3].

As the creep component of the cycle is increased by increasing the tensile dwell period or by reducing the strain rate in cycle; the failure mode of the material under the test also changes [4]. The failure modes observed can be categorized into three distinct regimes (Fig. 3). These are:

- (a) fatigue dominated,
- (b) fatigue-creep interaction and
- (c) creep dominated.

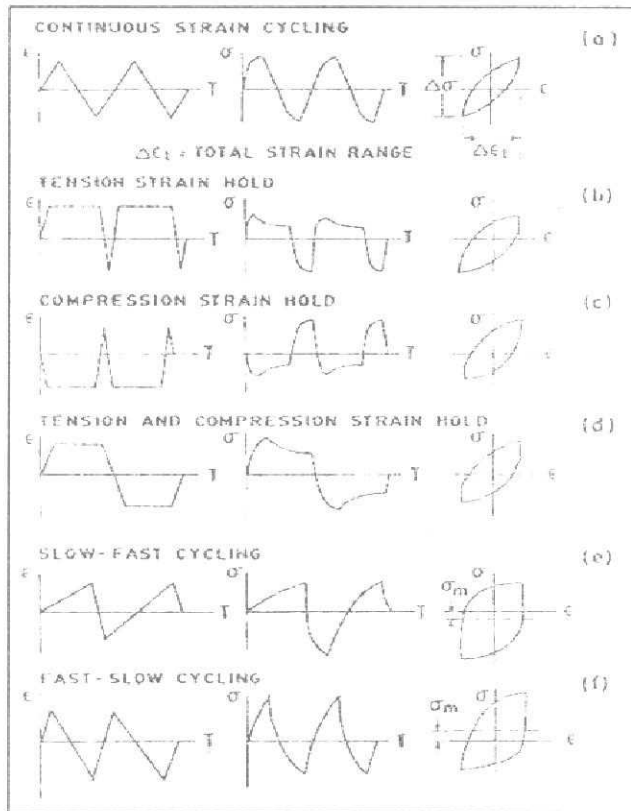


Fig.1: Typical waveforms for strain controlled fatigue testing

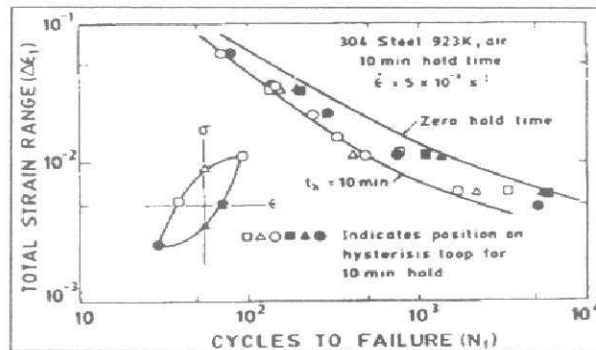
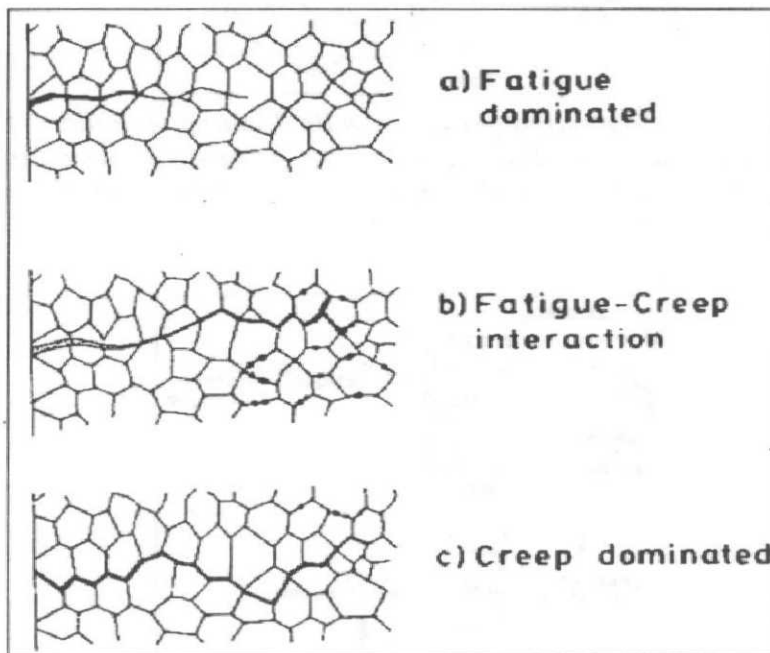


Fig.2: Influence of 10 min. hold position on fatigue life of type 304 stainless steel at 923 K [3]

Fatigue dominated failures arise due to the growth of surface fatigue cracks through the specimen, with no evidence of interaction with any creep damage (Fig. 3a). During creep-fatigue interactions, creep cavitation damage is found within the material in addition to surface fatigue damage. Fatigue and creep damage initially develop

independently and the likelihood of true interaction depends on the balance between them. In tensile hold time tests, on 316 stainless steel at elevated temperatures, it is found that initial fatigue crack growth rates are similar to those occurring under continuous cycling conditions as demonstrated by fatigue striation measurements. However, eventually the fatigue crack interacts with creep damage, resulting in accelerated crack growth, a reduction in endurance and creep-fatigue interaction failure, Fig. 3b. When such interaction occurs the failure path would become mixed (trans- plus inter-granular). Finally, under certain testing conditions, the creep component of the cycle dominates, and intergranular fracture due to the accumulation of grain boundary cavitation results (Fig. 3c), under these conditions there is no interaction with fatigue damage present.



*Fig.3: Schematic diagram of failure modes during creep-fatigue interaction testing [4].*

The creep-fatigue interaction failure can be described from two points of view [5]:

- (a) Influence of cyclic loading on cavitation damage and
- (b) Influence of cavitation on cyclic crack initiation and propagation.

Creep-fatigue failure can be either cavitation-damage dominated or crack-damage dominated. Conceptual mechanisms for each case was proposed by Raj [5]. These are illustrated in Figs 4 and 5. In the case of cavitation damage (Fig. 4), the imposition of cyclic loading enhances the rate of damage formation. It can be seen that the integrated

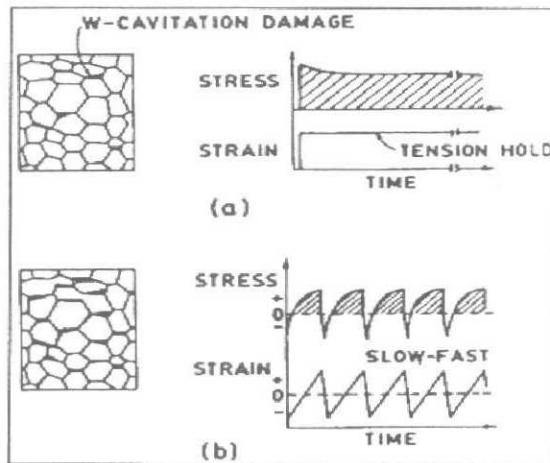


Fig.4: In a cavitation dominated failure, cyclic loading enhances the rate of damage accumulation. For example the integrated stress-time area is smaller for cyclic loading (b), than it is for monotonic loading (a), yet the damage is greater for cyclic loading [5].

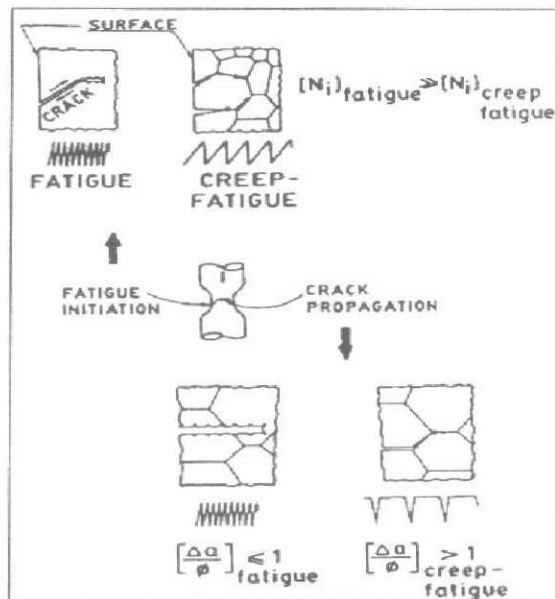


Fig.5: In a crack dominated failure, cavitation can accelerate either crack initiation or crack propagation.  $[N_i]_{fatigue}$  = number of cycles for crack initiation in a pure fatigue condition,  $[N_i]_{creep-fatigue}$  = number of cycles for crack initiation under creep-fatigue condition,  $\Delta a$  = crack advance per cycle and  $\phi$  = crack tip opening displacement [5].

stress-time area (Fig. 4) is smaller for cyclic loading than it is for monotonic loading, yet the cavitation damage is greater. The influence of cavitation damage on fatigue-crack initiation and propagation is illustrated in Fig. 5. Here cavitation may either enhance crack initiation or propagation. Experimental evidence indicates that in pure fatigue only one or two cracks are initiated, whereas in creep-fatigue many grain boundaries at surface develop cracks, and the largest among them propagates as the major crack. In the case of cavitation-enhanced crack propagation, the crack can grow by lengths much greater than crack-tip opening displacement due to the linkage of cavities ahead of the crack tip.

The above discussion outlines that there are three mechanisms of creep-fatigue interaction:

- (1) Cavitation damage enhanced by cyclic loading
- (2) Crack initiation enhanced by cavitation damage and
- (3) Crack propagation enhanced by cavitation damage.

These three mechanisms are shown schematically in Fig. 6 [5].

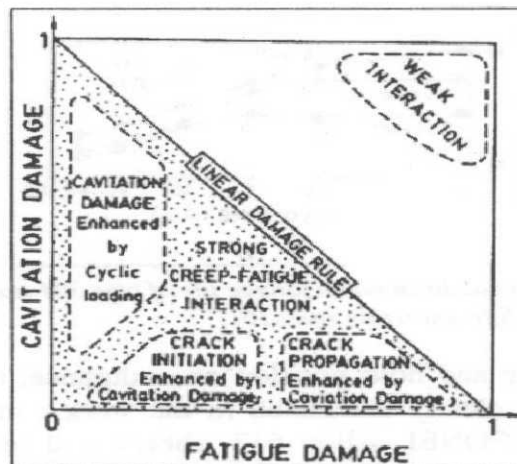


*Fig. 6: A schematic representation of how the three mechanisms of creep-fatigue interaction may lead to deviation from the linear damage rule [5].*

### ***Hold Time Effects***

The conditions which cause creep-fatigue interaction in various engineering materials are discussed below. There is now a large amount of information on austenitic stainless steels which indicate that the hold periods have an effect on fatigue life that is dependent not only on the ramp rate, position and length of hold in a cycle, but also on the microstructure. Figure 7 illustrates the combined influence of tensile strain hold periods, ramp strain rate and temperature on endurance of type 304 SS [6]. There is a clear reduction in life as a result of an increase in dwell period at elevated temperatures as a result of creep-fatigue interaction (Fig. 7a), whereas at sub-creep

(low) temperatures for small hold periods fatigue life seems to be rather independent of hold period. It appears that the fatigue life for type 304SS at 823 K is indicative of the transition between the low and high temperature hold time behaviour. The results shown in Fig. 7b also show a distinct influence on the ramp strain rate on hold time fatigue life; indicating that besides the creep damage accumulation during the hold time period a substantial part of the total damage would be generated during the loading and unloading periods as well.

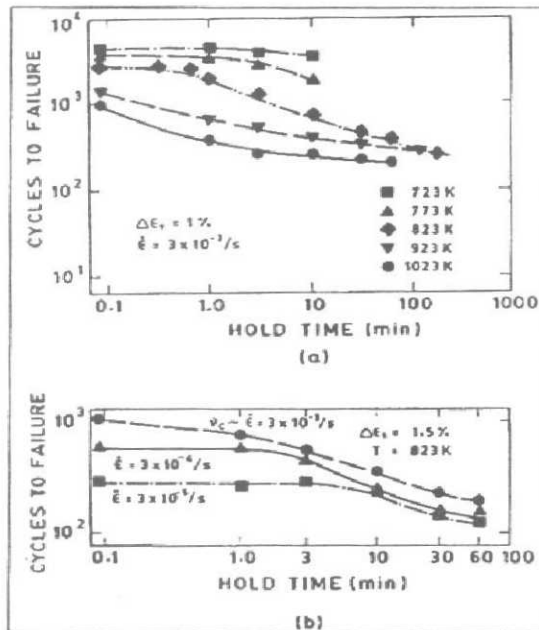


Fig. 7: The influence of tensile hold duration on fatigue life of type 304 stainless steel (a) for different temperatures, (b) for different strain rates [6].

The effects of hold time and hold position on endurance, cyclic deformation and fracture modes have been clearly elucidated in the work carried out by one of the authors on Alloy 617 (INCONEL Alloy 617, abbreviated to Alloy 617, is a solid solution strengthened wrought nickel base alloy) at 1173 K in helium environment [7]. Many interesting features involved in creep-fatigue interaction are discussed below using the results from this work.

From Fig. 8 it can be seen that, decreasing strain rate (increasing cycle time) caused only a small reduction in fatigue life in the continuously cycled tests [7]. Hold times at the tensile peak strain led to a pronounced reduction in life in comparison with continuously cycled tests of equal cycle duration. A compressive peak strain hold was also found to cause large reductions in life but its effect was slightly less than that of tensile hold. Equal hold periods both in tension and in compression yielded reduction factors which were very close to the continuous cycling data. It should be noted that fatigue life reduction increased continuously with an increase in hold time irrespective

of the type of hold conditions employed in a given cycle; no saturation of the reduction is evident.

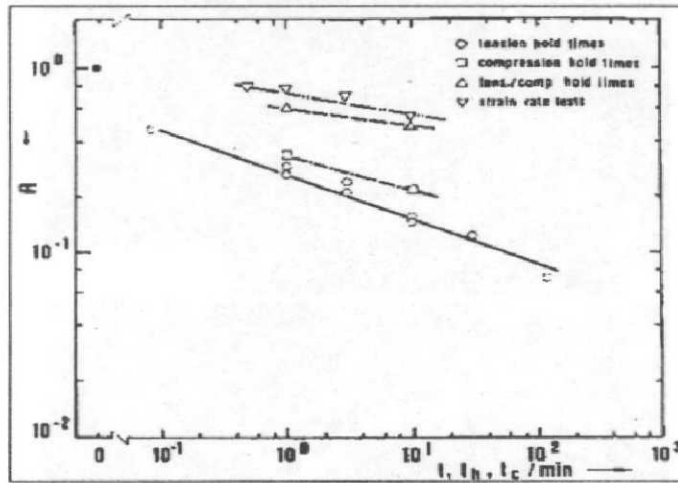


Fig. 8: The life reduction factor  $R$  against the cycle period in minutes for different loading conditions.  $R$  is defined as the ratio of  $N/N_f$ , where  $N$  is the fatigue life recorded for a given strain rate or wave shape and hold time and  $N_f$  is the reference life value for continuous cycling [7].

In the continuous cycling tests at all the strain rates, failure was transgranular with no indication of creep or oxidation damage was observed. In the 1 min tension hold time test, cracks initiated transgranularly by stage I shear cracking whereas crack propagation occurred by mixed mode. In the test with tensile holds of greater than 10 min crack initiation occurred intergranularly and propagation took place by mixed mode fracture. The compression hold tests displayed a dimple fracture similar to a tensile fracture accompanied by necking. The reduction in fatigue life which occurred when tensile hold periods are applied are principally due to the interaction between surface initiated fatigue crack and interior creep cavitation damage associated with grain boundary carbides. Figure 9a clearly illustrates the development of intergranular cavities (R-type) associated with grain boundary precipitates adjacent to the fracture surface in 1 min tension hold test. Figures 9b and 9c describe the cavity formation and cavity linkage on grain boundaries in the samples cycled with 10 and 120 min tension holds in the regions remote from the fracture surface. R-type cavities formed at grain boundaries were associated with second phase particles. Figure 9b clearly illustrates that the cavities on tensile boundaries quickly join up and initiate one or several microcracks which can propagate to form a macrocrack of the size of grain diameter.

The damage behaviour during the tensile hold period could be explained by characterizing the tensile stress relaxation behaviour as a function of time. A typical mid-life stress relaxation response curve for the 120 min tensile hold test is shown in Fig. 10. It can be seen that rapid relaxation down to half the maximum stress occurred in less than 1 s. Further, the inelastic strain rate ( $\epsilon$ ) associated with relaxation strain

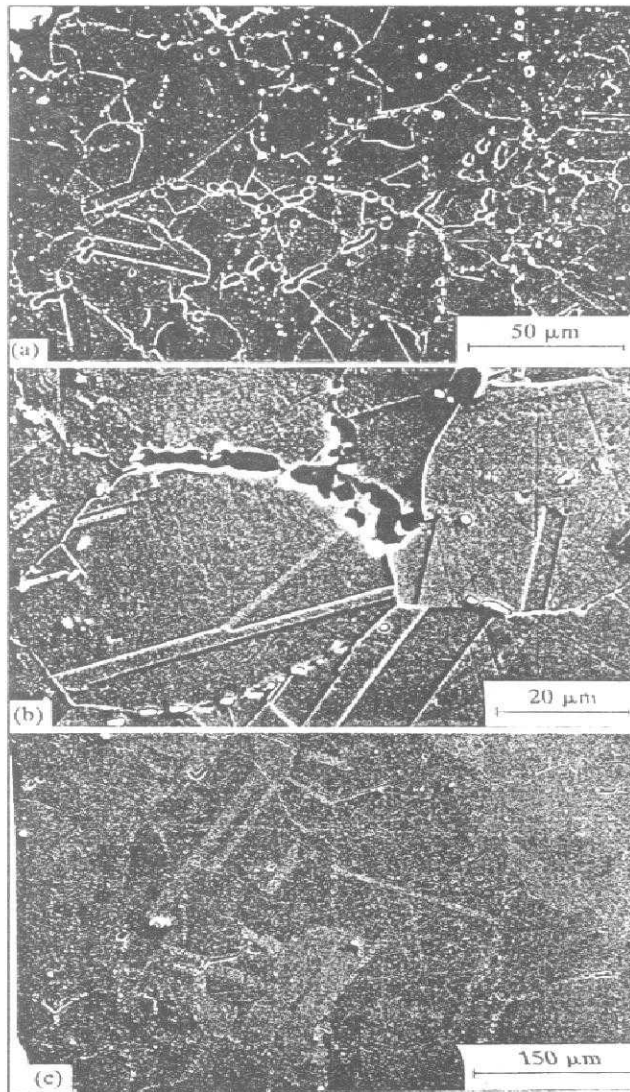


Fig.9: (a) Intergranular cavity damage adjacent to the fracture surface in Alloy 617 sample tested with 1 min. hold in tension (Cavities are associated with grain boundary precipitates); (b) cavity coalescence on grain boundary oriented at  $90^\circ$  to the loading axis (10 min. tension hold) and (c) Intergranular cavity damage in the sample subjected to 120 min tension hold [7]

continuously decreased with increasing hold time from approximately  $6.5 \times 10^{-4}$  to  $4 \times 10^{-9} \text{ s}^{-1}$ . It has been noticed that the inelastic strain rates found in the slow relaxation period during hold time tests are comparable to that of minimum creep rate data available from creep tests. It must be pointed out that the inelastic strain rates found in the rapid relaxation period correspond to those which are expected for precipitation-free matrix deformation, while those observed in slow relaxation period are typical for creep deformation. This comparative evaluation clearly indicates that during the tensile

hold period the build-up of tensile inelastic relaxation strain caused severe R-type cavitation damage observed within the bulk of the material. R-type creep cavities are known to form during tensile stress relaxation by clustering of vacancies at the junction between grain boundaries and second phase particles under the influence of tensile stress and probably grow by diffusional transport of vacancies or by deformation of grain matrix material.

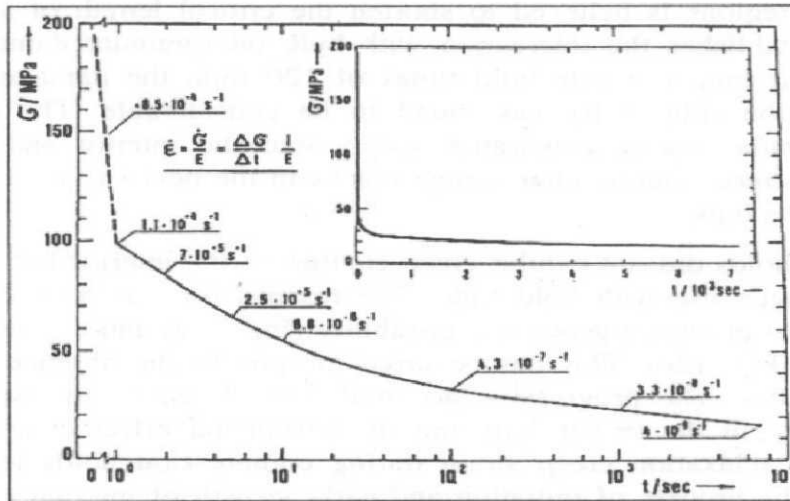


Fig. 10: Mid-life stress relaxation curve for Alloy 617 in a 120 min. tension hold test [7].

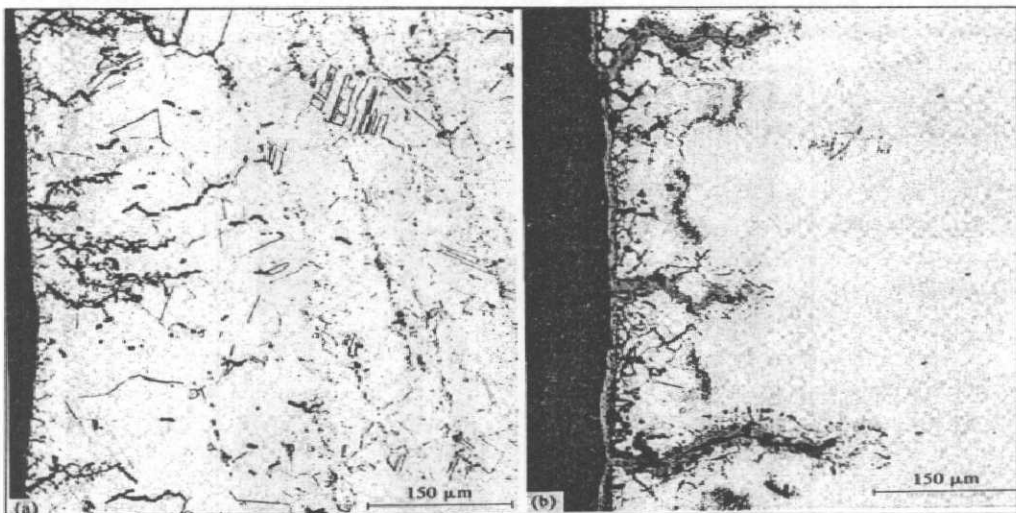


Fig.11: (a) Grain boundary wedge cracks in the near surface regions that are free from carbide precipitation (10 min. tension hold) (b) Thick oxide layer formed on the surface in 120 min. tension hold test (the crack faces of secondary cracks are also oxidized, and internal oxidation ahead of crack tip can also be seen) [7].

In addition to the bulk damage, a large number of grain boundary cracks were observed in the surface regions particularly when the tension hold times were more than 10 min (Fig. 11a). The formation of thick oxide scales (Fig. 11b) at the surface during longer hold times led to chromium depleted surface zones in which the carbide precipitates were dissolved. The loss of grain boundary carbides seems to have caused grain boundary sliding and enabled the formation of wedge cracks (Fig. 11b). Cracking in near surface regions is believed to shorten the critical length of surface fatigue cracks which establishes the interaction with bulk intergranular damage associated with carbides. At longer tensile hold times of 120 min, the damage due to grain boundary oxidation (Fig. 11b) was found to be considerable. The oxide-induced surface intergranular cracks penetrated deeply into the interior and merged with independently formed intergranular wedge cracks in the near surface regions and R-type cavities in the bulk.

Compression holds did not exhibit creep cavities in the interior but showed larger reduction in fatigue life with hold time. The reasons for this have been analyzed. Compression hold produced geometric instability (Fig. 12a) and consequently tensile necking failure (Fig. 12c). This has occurred in spite of the absence of significant tensile mean stress. The progressive accumulation of tensile inelastic strain with continued cycling in the tensile half and its detrimental effect compared with the accumulation of relaxation creep strain during compression holds leads to tensile fracture. Since the process of initiation and early growth of internal grain boundary cavities which give rise to interactive failures require both shear and normal tensile stresses across the grain boundary, bulk damage is unlikely to occur during the period of compressive stresses.

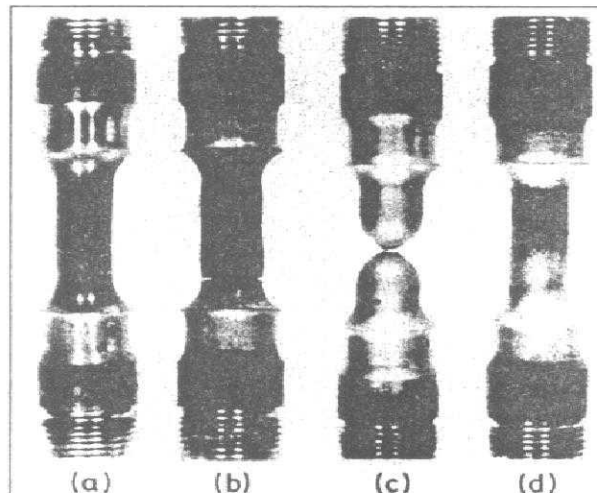
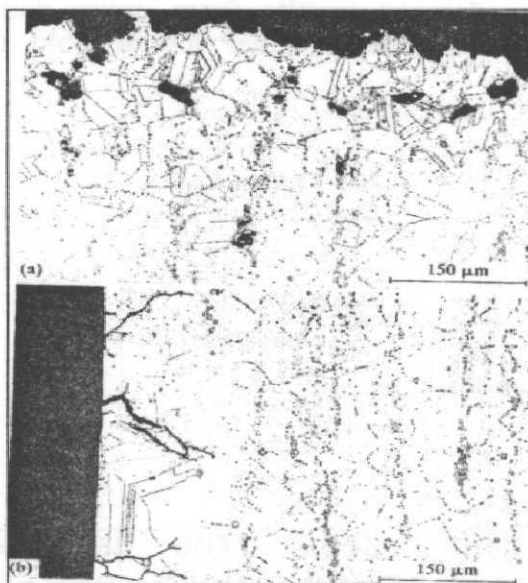


Fig.12: Photograph of broken specimen tested at strain rate =  $4 \times 10^{-3}$  s<sup>-1</sup>. (a) Continuous cycling (b) 10 min. tension hold (c) 10 min. compression hold and (d) 10 min. tension plus compression hold. Geometrical instability in the gauge portion of the samples subjected to tension only and compression-only holds can be clearly seen [7]

The optical micrographs presented in Fig. 13 illustrate the results for 5 min symmetrical hold tests. In contrast with the uniformly distributed intergranular cavitation damage in the specimen interiors of tensile hold tests, the cavity damage has been confined close to the fracture surface (Fig. 13a). No wedge cracks were seen in carbide depleted zone in the near surface regions (Fig. 13b) as opposed to the observation in tensile hold tests. In spite of fatigue-cavity damage interaction in the fracture zone, symmetrical holds exhibited better fatigue resistance than compression-only holds probably because of the non-existence of deformation ratcheting in the cycle.



*Fig.13: (a) Cavitation damage near the fracture surface in the 5 min symmetrical hold time test. (b) Carbide depleted zone in the surface regions and secondary cracks in this zone [7]*

It has been suggested that, if compressive hold periods follow the tensile hold periods, sintering of the cavities formed during the tensile hold period takes place during the compressive hold. In fact, the experimental findings of Majumdar and Maiya on type 304 stainless steel showed that symmetrical holds produced only transgranular failure contrary to the above observations of an interaction between the fatigue and cavity damage. It should be noted that the cavities in Fig. 13b are rather large, corresponding to the size of the grains, and were definitely not associated with grain boundary carbides as in the case of tensile holds. Furthermore, they were oriented at  $45^{\circ}$  to the stress axis. These observations indicate that these cavities nucleate and grow by irreversible shear deformation.

From the above results on Alloy 617, it has become apparent in longer hold time tests intergranular oxidation initiated intergranular cracks. Therefore a question arises, what would be the effect of oxidation on long term hold endurance? The true effect of the environmental influence could be assessed from comparative evaluation of tests

conducted in air and vacuum. The data from continuous cycling and hold time tests in air and vacuum conducted on type 304 stainless steel at 593 °C are presented in Fig. 14 [8]. This data clearly indicates the large differences in cycle life between continuous cycling data ( $\epsilon = 4 \times 10^{-3} \text{ s}^{-1}$ ) generated in air and high vacuum (1.3  $\mu\text{Pa}$ ). However, these differences tended to become minimal as the length of tensile hold time increased. Continuous cycling test in air and vacuum indicated transgranular fracture while larger hold time tests showed intergranular fracture. These results lead to an important conclusion that degradation in cyclic life under conditions that produce considerable intergranular damage results from creep damage rather than from environmental interactions. Therefore, under longer hold tests true creep-fatigue interaction results.

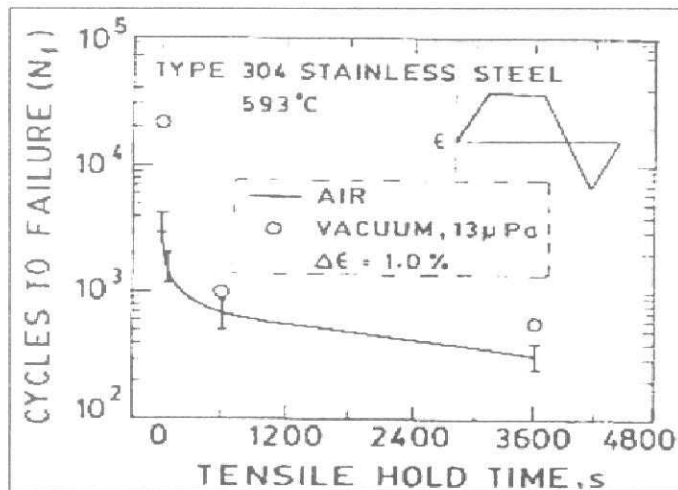


Fig. 14: Degradation of fatigue life resulting from tensile hold times becomes nearly the same for high vacuum and air environment as length of the hold period increases [8].

Strain range employed in the test and creep ductility have been identified as the two most parameters that exert influence on fatigue life and failure mode of several high temperature alloys [9]. From the compiled information on several ferritic steels (Fig.15), it is evident that the lower the creep ductility, the lower is the endurance. It can be seen that creep-fatigue interaction failures are predominant at relatively high strain ranges and high ductilities while creep dominated failures occur at low strain ranges, low ductilities and longer hold times. The requirement of both fatigue cracks and creep cavities shows that the interactive damage failure would cease either were absent. At low strain ranges the surface crack initiation becomes very slow relative to the development of internal creep damage and hence the failure becomes creep dominated. Both at high strain levels and rapid cycling conditions, failure becomes fatigue dominated as there is not enough time for the occurrence of creep damage. Below the fatigue limit, large cracks are not expected to initiate and microcracks generated at isolated places fail to link up and thus provide natural limit for creep-fatigue interaction. The accumulation of the information on failure modes during LCF

testing has been found indispensable in the construction of fatigue-creep interaction maps of the type shown in Fig. 16 for Type 316 SS [10].

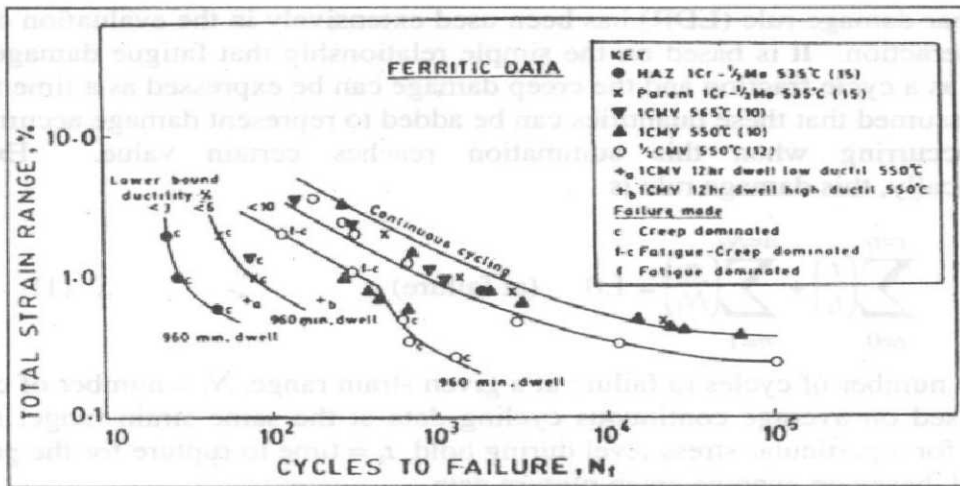


Fig. 15: Effect of ductility as endurance and fracture mode in low alloy ferritic steels [9].

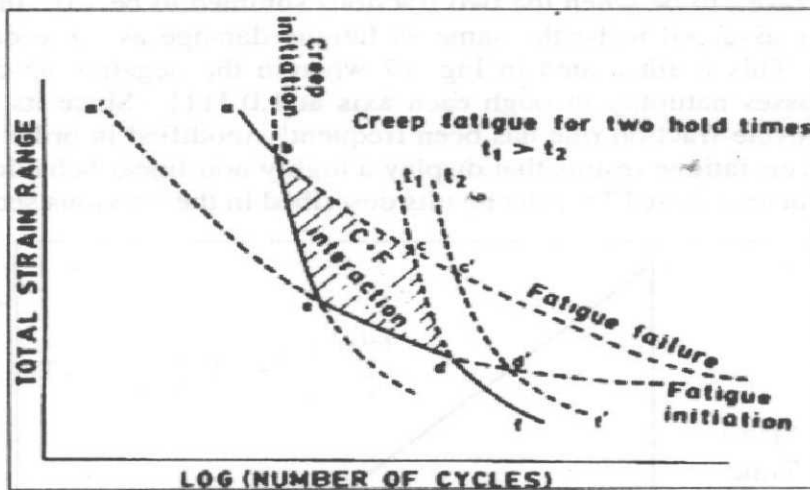


Fig. 16: Map showing the regions of different failure modes for Type 316 SS [10].

## CREEP-FATIGUE LIFE PREDICTION

### Linear damage (time and cycle fraction) rule

Development of a mathematical formulation for life prediction is one of the most challenging aspects of creep-fatigue interaction. It is complicated by the fact any proposed formulation must account for strain rate, relaxation at constant strain, creep at constant load and the difference between tension and compression creep, and must

be able to deal with disparate creep-fatigue response of different classes of materials used in high temperature applications.

The linear damage rule (LDR) has been used extensively in the evaluation of creep-fatigue interaction. It is based on the simple relationship that fatigue damage can be expressed as a cycle fraction and the creep damage can be expressed as a time fraction. It is also assumed that these quantities can be added to represent damage accumulation. Failure occurring when this summation reaches certain value. Expressed mathematically, this damage rule is

$$\sum_{t=0}^{t=t_f} \left( \frac{t}{t_f} \right) + \sum_{n=1}^{n=N_f} \left( \frac{n}{N_f} \right) = 1.0 \quad (\text{at failure}) \quad \dots (1)$$

where,  $n$  = number of cycles to failure at a given strain range,  $N_f$  = number of cycles to failure, based on average continuous cycling data at the same strain range,  $t$  = time increment for a particular stress level during hold,  $t_f$  = time to rupture for the particular stress level, based on average creep rupture data

The criterion for failure for linear time and cycle fraction rule for creep-fatigue interaction was taken to be when the two fractions summed to be 1.0. In other words, creep damage is assumed to be the same as fatigue damage as these damages to be added linearly. This is illustrated in Fig. 17 wherein the negative 45-degree failure criterion line passes naturally through each axis at 1.0 [11]. Since its inception the linear-time and cycle-fraction rule has been frequently modified in order to agree with experimental creep-fatigue results that display a highly non-linear behaviour, as shown in Fig. 18 [12] for Inconel 617 for the results described in the previous section.

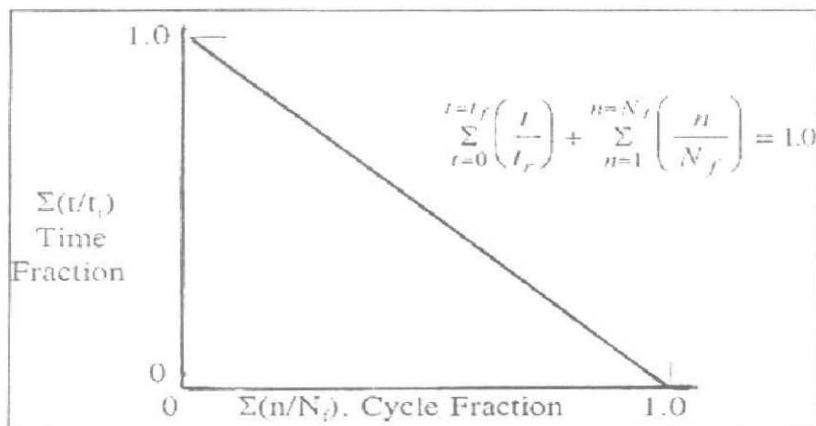


Fig. 17: Linear time- and cycle-fraction rule for creep-fatigue interaction [11]

There are several inherent deficiencies and potentially serious consequences of over- or under- design by using the classical linear-time and cycle-fraction rule for prediction of structural durability under high temperature creep-fatigue conditions

[11]. Monotonic tensile creep damage and fatigue damage mechanisms are quite different. Physically they do not add despite what an equation might imply. Creep-fatigue failure prone regions of a high temperature component are usually highly localized and overall deformation is limited by the greater bulk of the surrounding material. This condition leads to cyclically reversed loading for which the amount of monotonic (ratcheting) strain will remain quite small. These conditions bear little resemblance to what happens in a monotonic tensile creep rupture test wherein there is no reversal of straining, and large deformations are encountered before rupture occurs. In most high temperature service-loading conditions, the imposed creep is not always in the tensile direction, nor it is monotonic in nature like it occurs in conventional creep rupture testing used to establish the creep criterion. How to assess creep damage under compressive stress was a dilemma. Compressive creep rupture does not result in failures, so it was impossible to experimentally assess the validity of various assumptions concerning how compressive creep accumulated creep damage. In light of the above, it should become apparent that the superposition of the two in a linear fashion as prescribed by the linear-time and cycle-fraction rule is not physically viable approach.

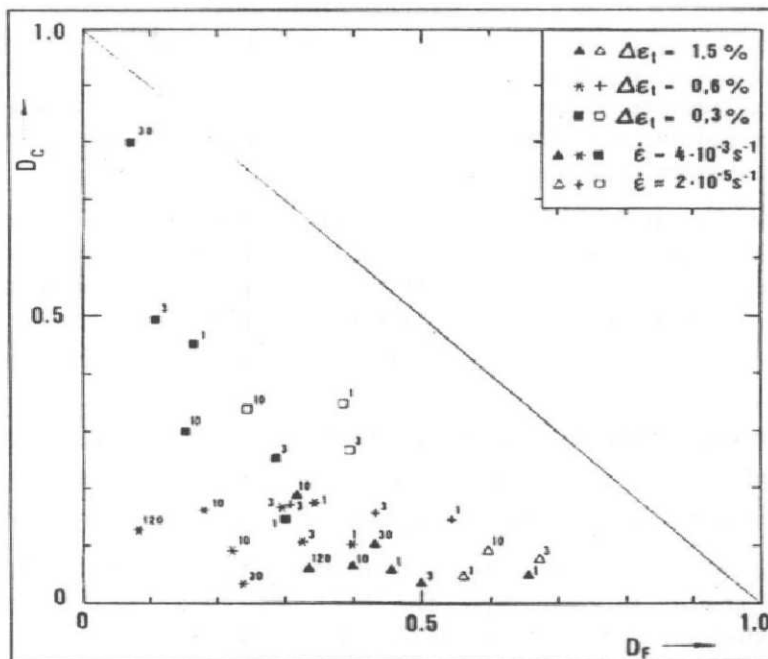


Fig. 18: Creep-fatigue interaction diagram for Inconel 617 alloy [12].

Stress is generally viewed as the governing variable for assisting creep damage, a structural analyst will have the tendency to improve the durability of his design by finding ways to lower the stress, compared to the strength of creep design curve. While this is mandatory in most instances, there are instances wherein achieving lowering stresses would not be advisable. For example, stress relaxation might be

viewed as a means of drastically decreasing the rate of creep damage accumulation, since that is what the time-fraction rule implies. As observed in the results of Inconel 617 superalloy (Fig. 10), as the stress relaxes during hold time, it converts non-damaging elastic strain into damaging creep strain. Regardless of what stresses may exist, creep damage cannot occur without creep strain. Without full understanding of the consequences of the selection, a designer may also be tempted to call out a lower strength heat of the alloy of choice to safeguard against accidental yielding without realizing that a weaker heat of material will simply undergo greater amounts of creep strain and hence greater amounts of physical creep damage. It is extremely important to recognize that stress per se does not cause creep damage, but rather creep strain does. Reliable predictive techniques are those which take into account the physical damage processes occurring during creep-fatigue deformation.

### Strain Range Partitioning

The method of SRP proposed by Manson and co-workers [13] focuses on inelastic strain present in a cycle and two directions of straining. Plastic flow is considered as the sum of all inelastic strain components which occur immediately upon application of stress (time independent in-elastic strain), while creep is considered as the sum of all time dependent components. The underlying bases for SRP are (i) in a strain cycle plastic flow and creep may occur separately or concurrently, and their interaction can strongly influence fracture behaviour (ii) the manner in which a tensile component of inelastic strain is balanced by a compressive component to close a hysteresis loop during a completely reversed straining determines the life.

In SRP, inelastic strain accumulated during one high temperature cycle is partitioned into four possible kinds of strain ranges depending on the direction of straining (tension or compression) and the type of inelastic strain accumulated (creep and plastic flow). Four inelastic strain ranges are defined as follows:

$\Delta\epsilon_{pp}$  = time independent tensile plastic strain reversed by compressive plastic strain (pp)

$\Delta\epsilon_{cc}$  = tensile creep strain reversed by compressive creep strain (cc)

$\Delta\epsilon_{pc}$  = tensile plastic strain reversed by compressive creep strain (pc)

$\Delta\epsilon_{cp}$  = tensile creep strain reversed by compressive plastic strain (cp).

A typical idealized classification of these four basic types of strain ranges is shown in Fig. 19 [14]. Fatigue relationships for each of these strain ranges are then experimentally established in the form of Coffin-Manson equation:

$$N_{jk} = A_{jk} \cdot \Delta\epsilon_{jk}^{\beta_{jk}} \quad \dots(2)$$

where  $j$  and  $k$  represent  $p$  or  $c$ . Experimentally established characteristic curves for different materials are shown in Fig. 20 [14]. Depending on the material each of the strain components has a different life-strain relationship.

For predicting life of a component the complex hysteresis loop representing the loading history, is broken down into components of the four loops and the partitioned

strain ranges are calculated as illustrated in Fig. 21. Only three of these four generic strain ranges can exist in a given hysteresis loop.  $\Delta\epsilon_{pc}$  and  $\Delta\epsilon_{cp}$  can not co-exist in the same loop.

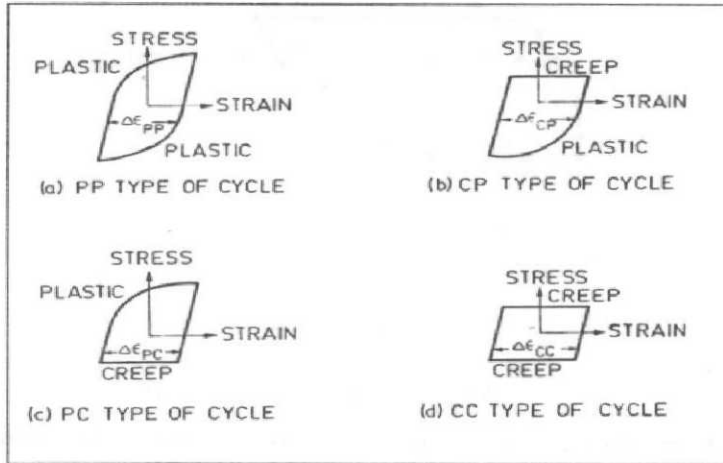


Fig.19: Idealised hysteresis loops for defining individual partitioned strain range-life relationships [14]

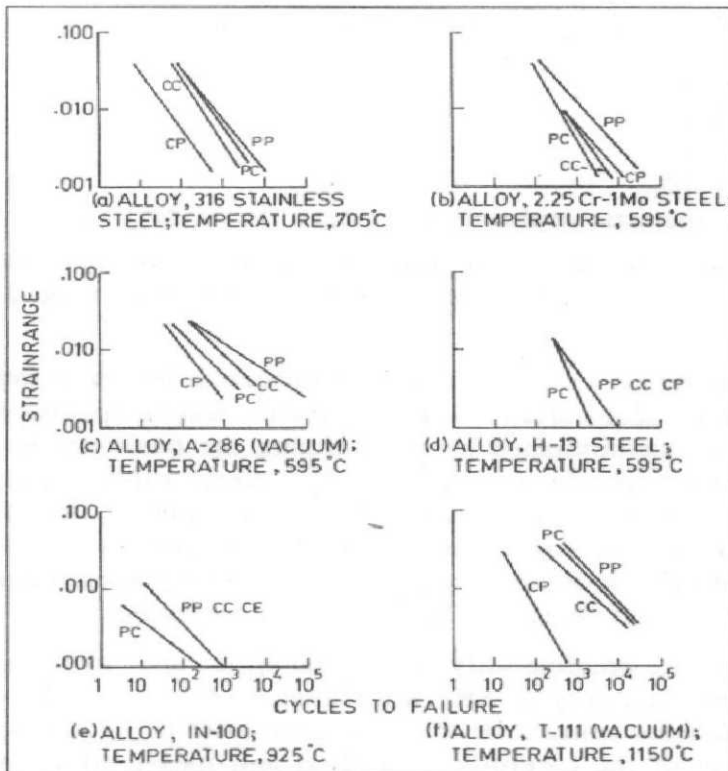


Fig.20: Partitioned strain range-life relationship for six alloys [14]

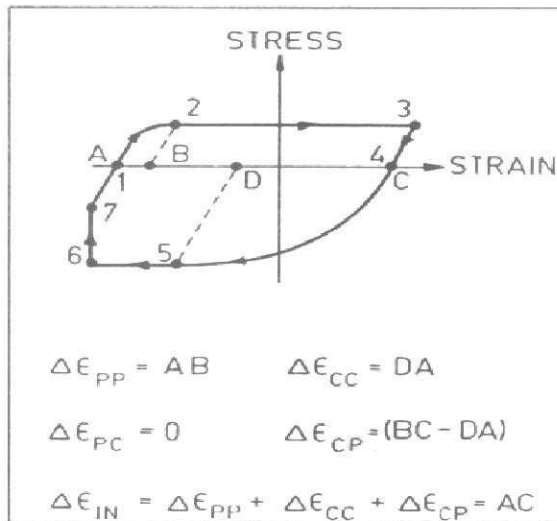


Fig.21: Defining partitioned strain range components of complex hysteresis loop [14].

The damage fractions resulting from each of the partitioned strain range components are summed up by an *interaction damage rule* (Fig. 17).

$$F_{pp} / N_{pp} + F_{cc} / N_{cc} + F_{cp} / N_{cp} \text{ (or } F_{pc} / N_{pc}) = 1 / N_{\text{predicted}} \quad \dots(3)$$

where

$$F_{pp} = \Delta \epsilon_{pp} / \Delta \epsilon_{IN}$$

$$F_{cc} = \Delta \epsilon_{cc} / \Delta \epsilon_{IN}$$

$$F_{cp} = \Delta \epsilon_{cp} / \Delta \epsilon_{IN}$$

$$F_{pc} = \Delta \epsilon_{pc} / \Delta \epsilon_{IN}$$

$$\Delta \epsilon_{IN} = \text{total inelastic strain range} = \Delta \epsilon_{pp} + \Delta \epsilon_{cc} + \Delta \epsilon_{cp} + \Delta \epsilon_{pc}$$

$N_{pp}$ ,  $N_{cc}$ ,  $N_{cp}$  and  $N_{pc}$  are the cyclic lives for each of the partitioned strain range components.  $N_{pp}$ ,  $N_{cc}$ ,  $N_{cp}$  and  $N_{pc}$  refer to points on life lines (Fig. 22) corresponding to  $\Delta \epsilon_{IN}$ .

SRP has been modified to account for the influence on creep-fatigue life of such parameters as heat to heat variations, environment, test temperature and stress etc . This modification is accomplished by normalizing the basic endurance relationships (DN-SRP) by factors based on unidirectional creep rupture ductility (for creep dominated *cc*, *cp* cycles) and on tensile ductility (for plastic flow dominated *pp*, *pc* cycles). In DN-SRP, it is assumed that ductility is a property which accurately reflects the various types of behaviour occurring during creep-fatigue interaction in wide range of materials. A total strain version of SRP has been presented.

The assessment of predictability of linear-time and cycle-fraction rule and comparison with predictability of SRP are shown in Fig. 23 for Incoloy 800 H [11]. The tests were conducted using total strain range control using appropriate strain hold-time tests. Because of the carefully controlled and measured variables and lack of extraneous variations due to heat-to-heat variations or structural analysis uncertainties, the figure unequivocally reveals the inherent inability of the LDR to accurately predict

creep-fatigue life times. The range of calculated lives covers a factor of 100 X (+5X / -20X). By comparison, the SRP reduced range of uncertainty to within a factor of only 4X. The improved accuracy is factor of 25X. The creep-fatigue life of 2.25Cr-1Mo has also been predicted very well by SRP.

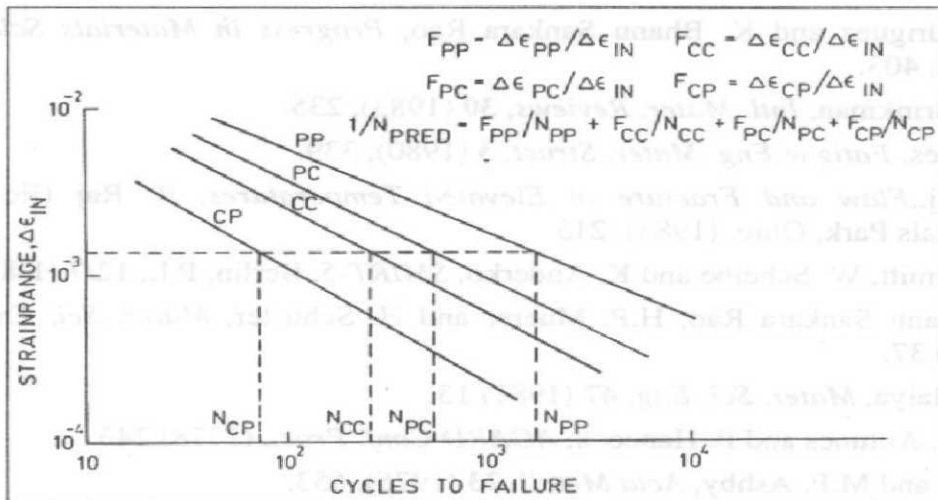


Fig.22: Definition of terms for an interaction damage rule [14].

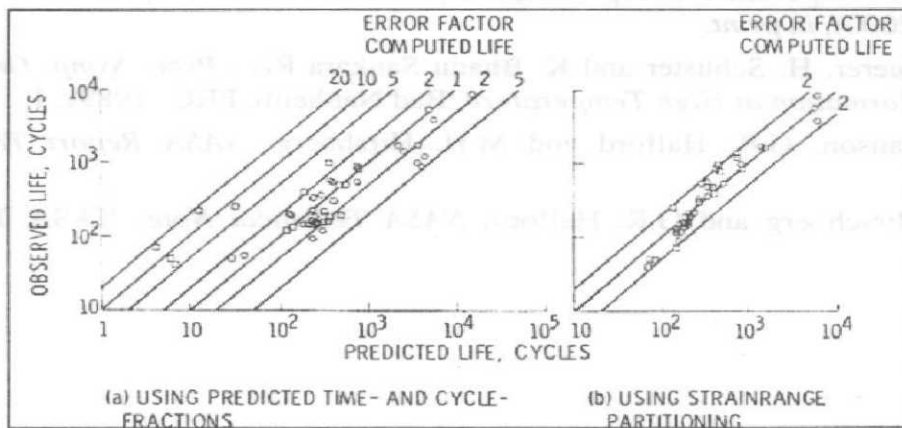


Fig.23: Assessment of predictability of linear time- and cycle-fraction rule and comparison with predictability of a strain based creep-fatigue life prediction (SRP) method [11].

### ACKNOWLEDGEMENTS

Authors are thankful to Shri R. Kannan, Scientific Officer, Mechanical Metallurgy Division, for many useful discussions and for the help in the preparation of the manuscript.

## REFERENCES

1. G.R. Halford, Creep-Fatigue Interaction, in Heat Resistant Materials, *ASM Specialty Hand Book*, J.R. Davis (Ed), ASM International, Materials Park, Ohio, (1997) 499.
2. P. Rodriguez and K. Bhanu Sankara Rao, *Progress in Materials Science*, **37** (1993), 403.
3. C.R. Brinkman, *Intl. Mater. Reviews*, **30** (1983), 235.
4. R. Hales, *Fatigue Eng. Mater. Struct*, **3** (1980), 339.
5. R. Raj, *Flaw and Fracture at Elevated Temperatures*, R. Raj (Ed), ASM, Materials Park, Ohio, (1983), 215.
6. R. Schmitt, W. Scheibe and K. Anderko, *SMIRT-5*, Berlin, P.L, 12/7 (1-8) 1979
7. K. Bhanu Sankara Rao, H.P. Muerer and H. Schuster, *Mater. Sci. Eng*, **A104** (1988) 37.
8. P.S. Maiya, *Mater. Sci. Eng*, **47** (1981) 13.
9. V.T.A. Antunes and P. Hancock, *AGARD Conf. Proc.*, (1978) 243.
10. R. Raj and M.F. Ashby, *Acta Metall*, **23** (1975), 653.
11. G.R. Halford, *A Critique of the Classical Linear Time – and Cycle-Fraction Rule for High Temperature Creep-Fatigue Life Prediction*, *Aerospace Materials Hand Book* (2000), *in print*.
12. H.P. Muerer, H. Schuster and K. Bhanu Sankara Rao, *Proc. Symp. On Strength and Deformation at High Temperature*, Bad Nauheim, FRG (1989), 1.
13. S.S. Manson, G.R. Halford and M.H. Hirshberg, *NASA Report TMX-67838* (1971).
14. M.H. Hirschberg and G.R. Halford, *NASA Technical Note*, NASA TND-8072 (1976).